



Journal of Advanced Research in Fluid Mechanics and Thermal Sciences

Journal homepage:
https://semarakilmu.com.my/journals/index.php/fluid_mechanics_thermal_sciences/index
ISSN: 2289-7879



Heat Propagation Across Turbocharger Unit with Variable Turbine Inlet Temperature

Mohd. Herzwan Hamzah^{1,*}, Azri Alias¹

¹ Faculty of Mechanical and Automotive Engineering Technology, Universiti Malaysia Pahang Al- Sultan Abdullah, Pekan, Pahang, Malaysia

ARTICLE INFO

Article history:

Received 28 June 2024

Received in revised form 23 September 2024

Accepted 1 October 2024

Available online 20 October 2024

Keywords:

Turbocharger; heat generation; forced induction system

ABSTRACT

Currently, issues about emission gains serious attention among the lawmakers and governments. Multiple regulation and enforcements have been applied to reduce the level of emission that released to the environment. Vehicle emissions have been identified as one of the major polluters thus forcing the carmakers to explore new technology to reduce the vehicle emissions. One of the technologies that have been preferred by the carmakers is the applications of forced induction system to the internal combustion engine. By using the forced induction system where currently turbocharger system is more often used compared to supercharger, two benefits can be achieved which are improvements of engine efficiency and engine size reduction. However, the ability of turbocharger unit to deliver compressed air can be affected by the amount of heat that travels along the turbocharger unit itself. In this paper, the effect of heat that originated from the exhaust gas that enters the turbine inlet towards the turbocharger performance was measured and analysed. An automotive turbocharger unit manufactured by Garrett Turbocharger model GT2056 was used in the study. The rotational speed is set between 20 000 rpm to 70 000 rpm and the temperature at turbine inlet is set between 40°C to 100°C. The parameters that measured are the temperature difference at internal turbine, internal bearing temperature difference, internal compressor temperature difference, turbine casing temperature difference, bearing housing temperature difference and compressor housing temperature difference. From the results obtained, it can be observed that the heat travels from turbine towards the compressor side through the conduction between the contacting parts between the turbine casing, bearing housing and lastly at compressor casing. The heat that arrives at the compressor side through the casing will give small effect to the air mass flow that delivered by the compressor.

1. Introduction

In the modern ages, the numbers of vehicles around the globe that powered by internal combustion engine is arising. As for example, statistics that created by the Ministry of Transportations Malaysia (MOT) stated that in 2022, total 720 658 units of new vehicles was registered in Malaysia [1]. Moreover, the MOT has forecasted that the number of total industry

* Corresponding author.

E-mail address: herzwan@gmail.com

<https://doi.org/10.37934/arfmts.122.2.102117>

volume forecast for 2024 until 2027 will show an increasing trend for at least 0.1% every year. The statistics indicate that the number of new vehicles registered is steadily high from year to year. Furthermore, majority of these registered vehicles are powered by internal combustion engines where the source of power for this engine is fossil fuel. One of the drawbacks of internal combustion engine usage is the production of exhaust emissions as by-products. This exhaust emission has a bad effect on human beings and at the same time harms the environment [2-4]. To overcome the problem, policy makers have enforced more stringent emission regulations in order to reduce the impact of emissions [5,6]. Hence, various technologies have been implemented in order to increase engine efficiency and at the same time decrease the engine emission level such as combustion cylinder deactivation (CDA), gasoline direct injection (GDI), variable valve timing and lift and many more [7-14]. Moreover, some manufacturers go for even greener solutions such as electric vehicle introduction and synthetic fuel [15-17]. Other than that, there are another alternative to cope with the regulations and at the same time lower the fuel consumption which is engine downsizing. The advantages of a small size engine include producing lower emissions, less mechanical losses, less pumping losses and also less weight [18]. However, small displacement engines may produce limited output due to limited amount of air that can be induced into the combustion chamber during the intake stroke. Thus, to overcome this problem, a forced induction system is fitted to the engine. A forced induction system generally consists of an air pump that pumps compressed air into the intake manifold. This air pump is either driven by exhaust gas or belting that is attached to the crankshaft pulley. A forced induction system that is driven by exhaust gas is known as a turbocharger and the system driven by belting is known as a supercharger. The advantages of forced induction system usage in an internal combustion engine are it will increase the degree of intake air boosting thus producing higher system efficiency [19]. A forced induction system also forces a higher amount of airflow that is being channelled into the intake manifold thus increasing the engine output [20].

The turbine of a turbocharger unit is driven by the exhaust gas that has a high temperature. While it contains a high amount of energy, this high exhaust gas temperature can affect turbocharger performance. The high exhaust gas temperature will cause heat propagation across the parts of the turbocharger. However, the common practice of turbocharger performance measurements ignores the heat transfer effect to the turbocharger performances [21-24]. Thus, since the heat transfer gives a significant effect on the turbocharger performance as stated by Gao *et al.*, [25], multiple researches have been conducted to evaluate the effect of heat transfer on the turbocharger performance.

Prévost *et al.*, [26] have conducted a study to develop a complete methodology to address turbocharger modelling based on corrected maps. In the study, the thermal transfer is characterised on two different turbocharger units where statistical analysis on multiple regression is used to establish the semi-empirical correlation. On the experimental part, the authors mounted the turbocharger on two different engine test benches consisting of 1200 cubic centimetre (cc) engine together with turbocharger waste gate. In the testing, the temperature and pressure at turbine and compressor inlet and outlet are measured. In the end of the study, the authors successfully developed a methodology to transform the turbocharger supplied maps. The methodology is based on the correlations that were established on a turbocharger gas stand by comparing a standard characterisation map with an adiabatic map. The correlations for heat transfer on the turbine side, compressor side and mechanical friction are obtained through semi-empirical regression. Additionally, the corrected isentropic efficiency map is determined for turbine and compressor side.

Heat transfer study and mechanical losses inside turbocharger unit also being conducted by Serrano *et al.*, [27]. In the study, the author conducted an experimental testing on an engine test bench to compare the output from the testing to a simulation of a turbocharged diesel engine. The testing is conducted using two different turbochargers (comes with water cooled system and without

water cooled system) which is coupled to a two-litre engine. The aim of the study is to observe the influence of turbocharger outlet temperature and predict the engine performance. The output from the study shows that the manufacturer's provided maps in hot conditions are adequate to predict all the variables at engine full loads except for turbine outlet temperature (TOT) and compressor outlet temperature (COT). This finding shows the importance in heat transfer model utilisation for the turbocharger performance testing. Moreover, utilisation of heat transfer model enables the determination of turbine and compressor outlet temperature without disturbance to the predictions of the other engine parameters.

Additionally, Serrano *et al.*, [6] also presented a methodology to obtain the heat transfer correlations through heat flux measurement between the different turbocharger parts. The author runs three different turbocharger unit on a continuous air flow test bench. The turbocharger unit is externally insulated to obtain the internal heat convective coefficient and correlations. The results obtained from the experiment is compared to the simplified lumped model to validate the methodology. At the end of the study, it is concluded that heat losses at turbine side build up while turbine enthalpy drop. However, the heat losses give significant impact only at low loads. Similar phenomenon also happens at compressor side where the adiabatic conditions can be treated at medium level. The heat transfer at compressor side will be intensify at compressor outlet since no heat will reach the compressor inlet.

Salameh *et al.*, [28] carried a study where the aim of the study is to generate the lump mass heat transfer model where every element of the turbocharger is treated as thermal mass. In the study, the author carried an experimental testing is to validate the generated model and also to indicate the effect of liquid cooling on the thermal transfer between the turbocharger parts. The experimental setup utilises is done on water cooled turbocharger which is mounted to a turbocharger test bench that utilises the air compressor as a gas source. The output from the study shows that the heat transfer model that generated can produce a new map at adiabatic conditions. The heat transfer model on the compressor side produces an efficiency map in adiabatic condition where this map can correct the efficiency that already mentioned by the supplier of the turbocharger. It is also stated that the heat transfer on the compressor efficiency gives higher impact on low turbocharger speed. However, while the turbocharger speed enters high speed region, heat transfer gives lower effect on the compressor efficiency even the amount of heat flux increases. This is because the mechanical power exchange is rising even more and make the heat transfer insignificant.

In this study, an automotive turbocharger is mounted on the gas stand test rig and operated by compressed air as energy source. In the study, heat source is supplied to the turbocharger unit by an electrical heater that heats up the air that enters the turbine. The aim of the study is to observe the heat propagation that started from turbine side and then later propagates to the other part of turbocharger unit. The temperature of the turbine inlet and the turbocharger speed will be varied and the temperature difference at significant point will be recorded.

2. Methodology

The experiment was conducted using a turbocharger gas stand test rig. The complete schematic diagram of the turbocharger gas stand test rig was shown in Figure 1. The turbocharger gas stand test rig used in the experiment consists of a compressed air stored inside a pressurised tank. The pressurised air is channelled to the turbocharger unit through a piping. The flow rate was controlled using an air valve that was mounted just after the compressed air tank. A heater was mounted at the pipeline just before the compressed air enters the turbocharger unit. The temperature of this heater is controlled by a control unit.

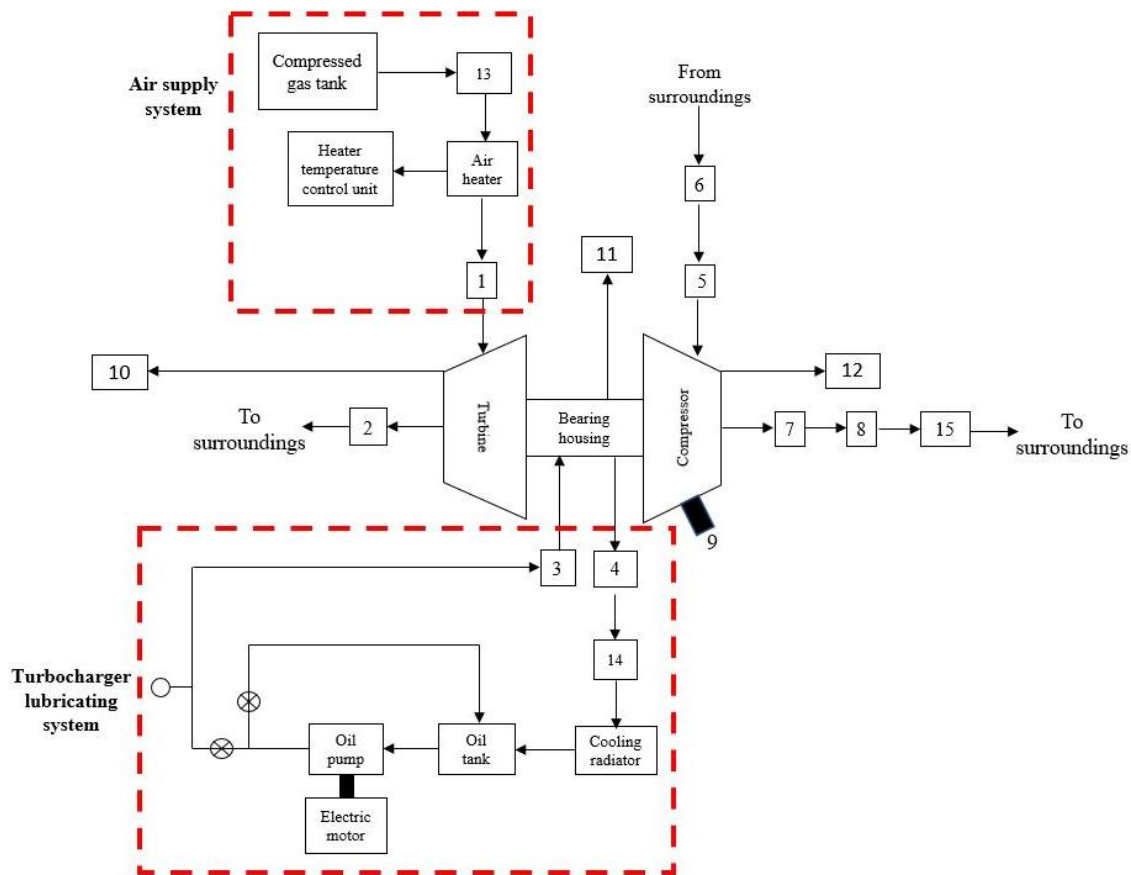


Fig. 1. Turbocharger test rig schematic diagram

The turbocharger that was used in the experiment is from Garrett Turbocharger and the model used was GT2056. This turbocharger was mounted to the compressed air piping using a custom mounting. A speed sensor was mounted to the turbocharger compressor side to measure the turbocharger speed. The speed was determined by measuring the speed of the compressor wheel tip. The speed of the turbocharger was varied by controlling the flow rate of the air that enters the turbine casing.

A lubricating system was equipped to the turbocharger system to provide the lubrication purpose. It consists of a positive displacement gear pump that provides the pressurised lubricating oil. The gear pump was driven by a three-phase electric motor that act as an actual engine drives the pump. The motor rotates at a constant speed of 1492 rpm. The electric motor is connected to the pump by a flexible coupling. The pressurised oil was pumped into the bearing housing to lubricate the turbocharger bearing. The pressure generated by the gear pump was controlled by a valve mounted at the gear pump outlet. The heated lubricating oil that comes out from the bearing housing was cooled using a cooling radiator and fan.

A number of thermocouples, pressure transducer and mass flow-rate sensors were mounted to a specific point at the test rig. The listing of the sensors that used in the test rig was listed in Table 1. The numbers shown in the figure denotes the thermocouple, mass flow sensor and pressure transducer that are mounted to measure the required data. Several data collected during the experiment need to be processed by the data processing unit. The measured data signal will be processed by the data acquisition unit (DAQ) and the results will be shown on the computer screen. The DAQ system consists of one unit of power supply cable, signal-processing unit and USB cable that is connected to the computer.

Table 1
List of mounted sensors

Number	Parameters
1	Turbine inlet temperature
2	Turbine outlet temperature
3	Lubricating oil inlet temperature
4	Lubricating oil outlet temperature
5	Compressor inlet pressure
6	Compressor inlet temperature
7	Compressor outlet temperature
8	Compressor outlet pressure
9	Turbocharger speed
10	Turbine outer casing temperature
11	Bearing housing outer temperature
12	Compressor outer casing temperature
13	Turbine inlet mass flow
14	Lubricating oil flow meter
15	Compressor outlet mass flow

The experiment was conducted referring to SAE J1826-Turbocharger Gas Stand Test Code and SAE J922-Turbocharger Nomenclature and Terminology as reference. The environment for testing is in the lab environment. The gas that used in the experiment is compressed air. Since the wastegate of this turbocharger is internally built, the wastegate valve is closed during the experiment testing. The oil pressure that used for lubrication is set at constant pressure at 3.5 bar. The turbocharger is tested with variable heat temperature applied to the air that enters the turbocharger. The data that was manipulated during the experiment is turbocharger speed and the turbine inlet temperature. The compressor inlet temperature remains at room temperature. The speed range of the turbocharger was between 20 000 rpm to 70 000 rpm with 10 000 rpm increment and the temperature of the turbine inlet is varied between 40°C to 100°C. The measurement data is taken after the temperature and mass flow of the compressor outlet is stabilised after one minute. The testing is repeated for each turbine inlet temperature and turbocharger speed ten times for data consistency. The data is determined by measuring the temperature difference between turbine inlet and outlet, the temperature difference between bearing housing inlet and outlet, and also the temperature difference between compressor housing inlet and outlet.

3. Results

Figure 2 shows the turbine side internal temperature difference. This temperature is measured by determining the difference between inlet and outlet temperature of the turbine side. The purpose of measuring the temperature is to investigate the amount of air temperature drop inside the turbine housing. This temperature difference value will be used to measure the amount of heat loss inside the turbine housing. The negative sign shows the temperature drop between the turbine outlet and inlet, where the temperature at turbine outlet is lower compared to the turbine inlet. From the graph, it can be calculated that the temperature difference when the air inlet temperature is set at 40°C is higher compared to conditions where no heat is exerted to the turbine inlet by 14%. When the temperature at turbine inlet is increased to 50°C, temperature difference is 76% higher compared to 40°C. Later, when the temperature at the turbine inlet temperature is increased to 60°C, the temperature difference is 44% higher compared to the difference when the turbine inlet is at 50°C. Next, as the turbine inlet temperature increase to 70°C, the temperature is 32% higher compared to the 60°C. When the turbine inlet temperature reaches 80°C, the temperature difference is 27%

higher for 80°C compared to the 70°C. While the turbine inlet temperature keeps rising until it reaches 90°C, the temperature difference is 22% higher compared to the previous temperature and lastly when the temperature is at 100°C, the temperature difference is 16% higher.

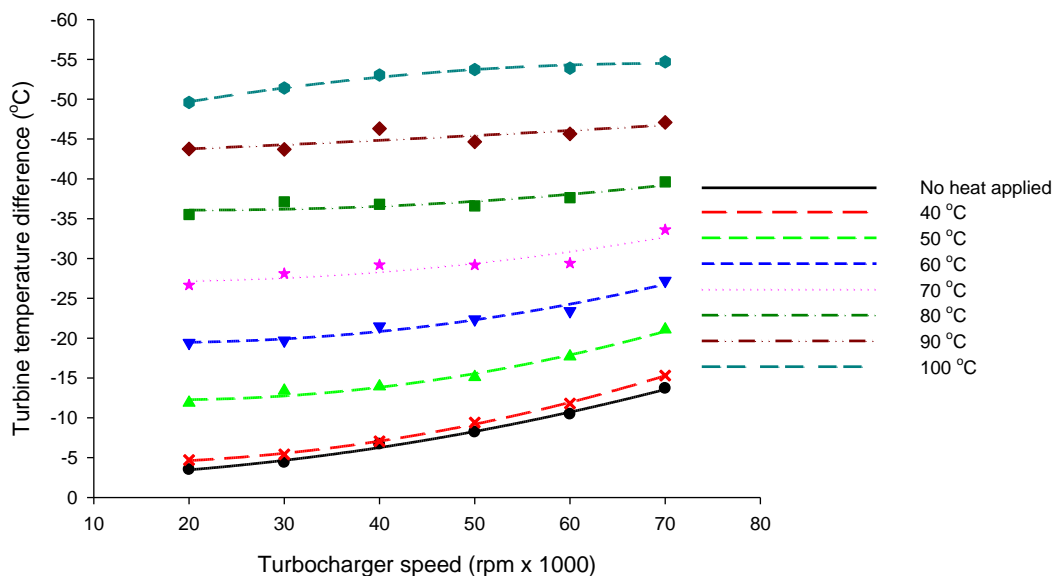


Fig. 2. Graph of turbine internal temperature difference versus turbocharger speed at different turbine inlet temperature

The percentage of difference between area under the curve for every turbine inlet temperature shows significant pattern where the figure shows decreasing pattern. This condition shows that for every turbine inlet temperature increment, the temperature difference between turbine outlet and turbine inlet is decreasing. This condition indicates that when the turbine inlet temperature is increased, the amount of energy that exit through the turbine outlet is decreased for every turbocharger speed. This means that, instead of the energy exits the turbine outlet, it is used as a work to rotates the turbine wheel. Some of the energy also lost to the environment from the turbine casing and some of the heat is transferred to the bearing housing and turbine wheel.

Figure 3 shows the temperature difference at turbine outer casing at different turbine inlet temperature while the turbocharger speed increased. The turbine outer casing temperature is measured by determining the temperature difference before and after the heat applied to the turbine inlet. From the graph, it can be determined that when the heat is applied to the turbine inlet at 40°C, the turbine outer casing temperature difference is 5693% higher compared to the temperature difference at the conditions where no heat is applied to the turbine inlet. When the temperature at turbine inlet is increased to 50°C, the temperature difference is 25.47% higher compared to the temperature at 40°C. Next, when the turbine inlet temperature is increased to 60°C, the turbine outer casing temperature difference is 28.72% higher compared to the temperature difference at 50°C. While the turbine inlet temperature is increased to 70°C, the temperature difference at outer turbine casing is 12.16% higher compared to the temperature difference at 60°C. Moreover, when the turbine inlet temperature is increased to 80°C, the temperature difference at turbine outer casing is 12.24% higher compared to the temperature difference at 70°C. Additionally, when the turbine inlet temperature is at 90°C, the turbine outer casing temperature is 8.96% higher compared to the temperature difference at 80°C. Finally, when the turbine inlet temperature is at 100°C, the turbine outer casing temperature is 8.58°C higher compared to the temperature difference at 90°C. From Figure 3, it can be observed that the temperature difference at the turbine outer casing shows increasing trends when the temperature at turbine inlet is increased. It indicates

that the amount of heat that travels to the casing of the turbine and next to the environment is increased when the temperature at turbine inlet is increased. Other than that, referring to the amount of temperature difference inside the turbine casing as shown in Figure 2, while the temperature of the gas that exits the turbine outlet is decrease, some of the heat is being transferred to the casing of the turbine due to the temperature difference. These conditions cause the temperature increment at the turbine casing as the temperature of the turbine inlet is increased.

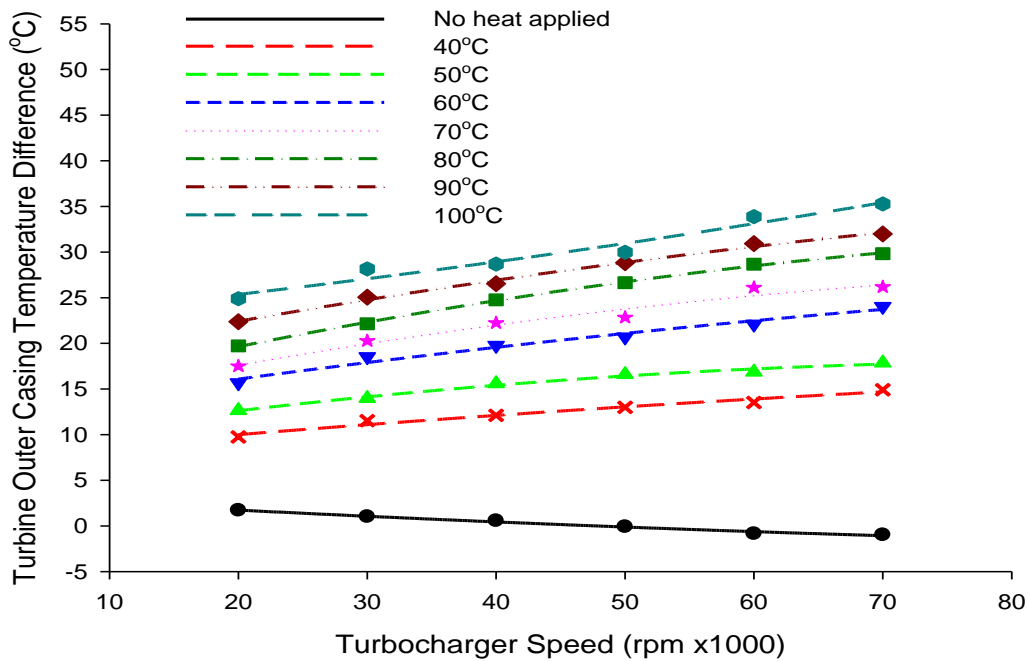


Fig. 3. Graph of turbine outer casing temperature difference versus turbocharger speed at different turbine inlet temperature

Figure 4 shows the compressor temperature difference when the turbine inlet temperature is varied and the turbocharger speed is increased. The temperature difference at compressor side is determined by measuring the difference between the compressor outlet and inlet. From the graph, it can be calculated that when heat is exerted to the turbine inlet at 40°C, the compressor temperature difference is 1% higher compared to no heat is exerted. While turbine inlet temperature is increased to 50°C, the compressor temperature difference is 3% higher from the difference at 40°C. Continuously, as the turbine inlet temperature is increased to 60°C, the temperature difference at compressor side is 2% higher compared to the difference at 50°C. When the turbine inlet temperature reaches 70°C, the temperature difference at compressor side is 1% higher compared to the difference at 60°C. Next, when the temperature at turbine inlet is raised to 80°C, the temperature difference is 2% higher compared to the difference at 70%. However, when the temperature at turbine inlet is 90°C, the temperature difference is slightly drop compared to the difference at 80°C by 0.2%. Finally, when the temperature at the turbine inlet is 100°C, the temperature difference at compressor side is 0.8% higher compared to the difference at 90°C. From Figure 4, it can be observed that when the for each different temperature that applied to the turbine inlet, a significant variations of internal temperature difference can be observed inside the compressor housing. The trend that shown from the graph shows that when the temperature of the turbine inlet is increased, the temperature difference inside the compressor housing is increased together with the turbocharger speed increment. This trend also shows that some of the heat from the turbine will travel across the bearing housing before reach the compressor side during turbocharger operations.

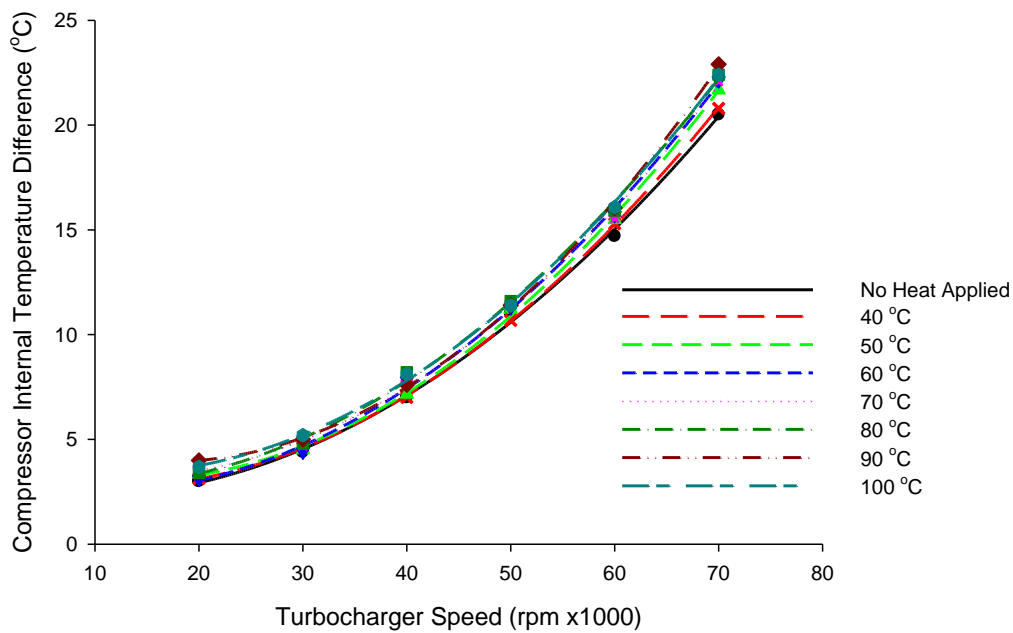


Fig. 4. Graph of compressor internal temperature difference versus turbocharger speed at different turbine inlet temperature

Figure 5 shows the temperature difference at the compressor outer casing when the turbine inlet temperature is varied and the turbocharger speed is increased. This temperature difference is determined by measuring the temperature difference at the surface of the compressor casing before the heat applied to the turbine inlet and the turbocharger running, compared to the temperature at measurement point during the experiment is conducted. From the graph, it can be calculated that when the turbine inlet temperature is set to 40°C, the temperature difference is higher compared to the temperature when no heat is applied to the turbine inlet by 2.14%. When the turbine inlet temperature is raised to 50°C, the temperature difference at compressor outer casing is 16.06% higher compared to the temperature difference at 40°C. Next, when the temperature at turbine inlet is at 60°C, the temperature difference at the outer compressor casing is 14.76% higher compared to the temperature difference when the turbine inlet temperature is at 50°C. Moreover, when the turbine inlet temperature reaches 70°C, the temperature difference at compressor outer casing is 9.65% higher compared to the temperature difference at 60°C. While the temperature continuously increases until 80°C, the temperature difference at the compressor casing is 3.82% higher compared to the temperature difference at 70°C. Other than that, when the temperature of the turbine inlet is set at 90°C, the temperature difference at compressor outer casing is 4.12% higher compared to the difference at 80°C. Finally, when the turbine inlet temperature is at 100°C, the temperature difference at the compressor outer casing is 5.86% higher compared to the temperature difference at 90°C. From Figure 5, it can be observed that for every turbine inlet temperature increment, there is significant increase of the compressor outer casing temperature difference together with turbocharger speed increment. This can be related to the amount of heat that being released to the environment due to the temperature increase inside the compressor casing. Similar to that, this figure also can be related to the Figure 4 where the temperature inside the compressor casing is increased when the temperature at the turbine inlet is increased. However, the temperature difference at the outer compressor casing is less than the temperature difference inside the turbocharger casing.

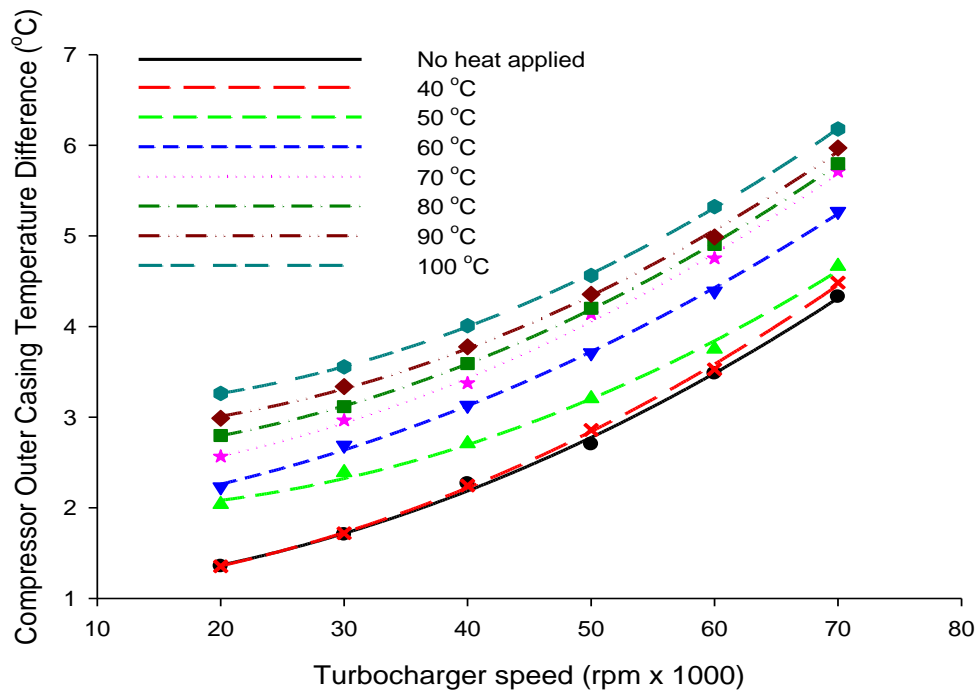


Fig. 5. Graph of compressor outer casing temperature difference versus turbocharger speed at different turbine inlet temperature

Figure 6 shows the lubricating oil temperature difference at different turbine inlet temperature while the turbocharger speed is increased. The temperature is determined by measuring the difference between the oil outlet temperature and oil inlet temperature. From the graph, it can be seen that when the heat is applied at turbine inlet at 40°C temperatures, the temperature difference at bearing housing is 0.47% higher compared to condition where no heat applied. When the temperature at turbine inlet is increased to 50°C, the temperature difference is only 0.01% higher compared to the difference at 40°C. However, when the temperature at turbine inlet is increased to 60°C, the temperature difference is 0.08% higher compared to the temperature difference at 50°C. While the temperature at turbine inlet reaches 70 °C, the temperature difference at bearing housing is 0.69% higher compared to temperature difference at 60°C. Moreover, as the temperature at turbine inlet is raised to 80°C, the temperature difference is 1.97% higher compared to the difference at 70°C. When the temperature then is raised to 90°C, the temperature difference is 2.60% higher compared to the difference at 80°C. Finally, when the temperature at turbine inlet reaches 100°C, the temperature difference is 1.52% higher compared to the difference at 90°C. From the trends that shown in the Figure 6, it can be observed that the temperature difference for the lubricating oil when the turbine inlet temperature is varied shows only small differences where the highest difference is only 2.6%. Based on the results that shown in Figure 6, the variations of temperature at the turbine inlet only have small impact on the lubricating oil change. Moreover, most of the temperature difference is caused by the frictional force that occurs between the rotating shaft and the bearings inside the bearing housing.

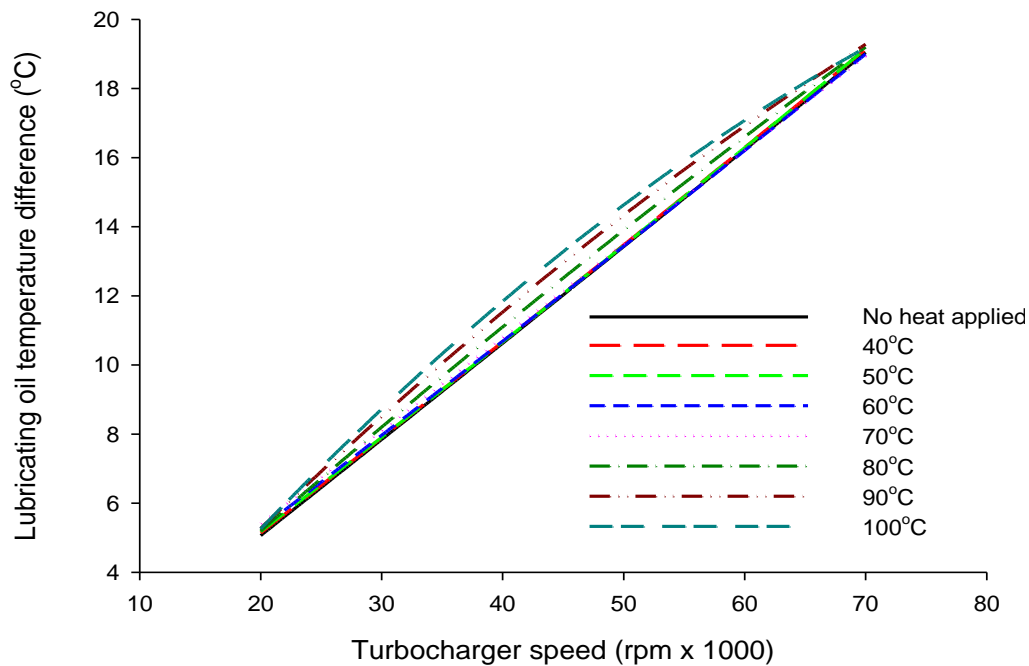


Fig. 6. Graph of oil temperature difference versus turbocharger speed at different turbine inlet temperature

Figure 7 shows the temperature difference measured at the outer bearing housing casing versus turbocharger speed at varied turbine inlet temperature. This temperature difference was measured by determining the temperature at the outer surface of the bearing housing before and after the turbocharger running at several speed and turbine inlet temperature. From the graph, it can be determined that when the turbocharger turbine inlet temperature is set at 40°C, the temperature difference at outer bearing housing is 3.7% higher compared to the temperature difference when no heat applied to the turbine inlet. While the temperature at the turbine inlet is increased to 50°C, the temperature difference at outer bearing housing is 4.9% higher compared to the temperature difference at 40°C. Moreover, when the temperature at the turbine inlet reaches 60°C, the temperature difference at outer bearing housing is 14.5% higher compared to the temperature difference at 50°C. Next, when the turbine inlet temperature is at 70°C, the temperature difference at outer bearing housing is 1% higher compared to the temperature difference when the temperature at turbine inlet at 60°C. Additionally, when the temperature of turbine inlet is at 80°C, the temperature difference is 1.5% higher compared to the temperature difference at 70°C. Other than that, when the temperature at turbine inlet is 90°C, the temperature difference at outer bearing housing is 1.9% higher compared to the temperature difference. Finally, when the temperature at turbine inlet reaches 100°C, the temperature difference at outer bearing housing is 1.7% higher compared to the temperature difference at turbine inlet temperature at 90°C. From the figure, it can be observed that while the temperature of the turbine inlet is increased, the temperature of the outer bearing housing is also increase. The temperature differences between each bearing housing temperature ranges from 14.5% to 1%. From the trends, it can be observed that the temperature difference of this part yields the second highest temperature difference in the three major parts of the turbocharger which is turbine and compressor casing. Moreover, this figure also shows that the bearing housing parts will emits the heat from its outer surface higher compared to the amount of heat that absorbed by the lubricating oil that exits from the inside of the bearing housing.

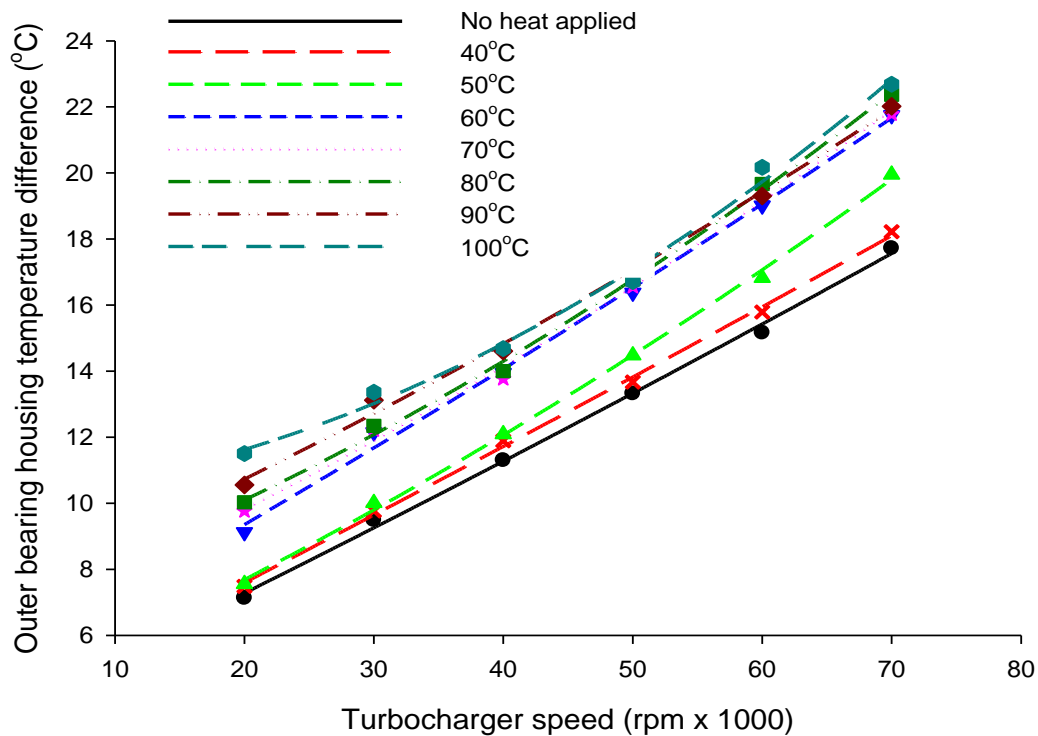


Fig. 7. Outer bearing housing temperature difference versus turbocharger speed at different turbine inlet temperature

Figure 8 displays the temperature difference across the turbocharger unit starting from turbine side, bearing housing side and finally at compressor side. Six measurement points was taken which is turbine internal temperature difference, turbine outer casing temperature difference, lubricating oil temperature difference, bearing housing outer temperature difference, compressor internal temperature difference and compressor outer casing temperature difference. Figure 9 and Table 2 describes the turbocharger components that measured for temperature difference. From the figure, it can be observed that the temperature difference at turbine side will increase with the turbine inlet temperature increment due to energy conversion. Moreover, the temperature difference at turbine outer casing temperature will also increase with the turbine inlet temperature increment. However, observing the temperature difference at lubricating oil temperature difference, the temperature difference is very small which is unnoticeable where the Figure 6 can be referred. It shows that the heat will not be able to travel through the internal part between turbine side and internal bearing housing part of the turbocharger, due to the existence of turbine backplate inside the turbine side, just behind the turbine wheel. This backplate have a void air-space that prevents the contact between the turbine wheel and the bearing housing, preventing the heat transfer process happening through the conduction between the internal turbine to the internal bearing housing. Moreover, observing the trends of temperature difference at bearing housing outer temperature difference. There is temperature difference increment corresponds to the variable temperature difference at turbine inlet. This indicates that the heat will travel through the bearing housing outer casing instead of travelling through the internal parts of the turbocharger unit. However, some of the heat that travelling through the casing may escape to the environment through the convection process before it reaches the compressor casing. Next, the temperature difference at internal compressor shows the increment corresponds to the turbine inlet temperature increment. At constant speed, the temperature difference that generated inside the compressor casing should be constant. However, as shown in Figure 8, there are temperature difference variations corresponds to the turbine inlet temperature increment. This indicates that the temperature from the bearing housing affects the

temperature difference at internal compressor where the heat that reach the compressor side will combine with the heat that generated by the air compression inside the compressor itself. Finally, the temperature variations at the compressor outer casing will be vary according to the temperature inside the compressor and also the temperature that reaches the outer casing from the bearing housing.

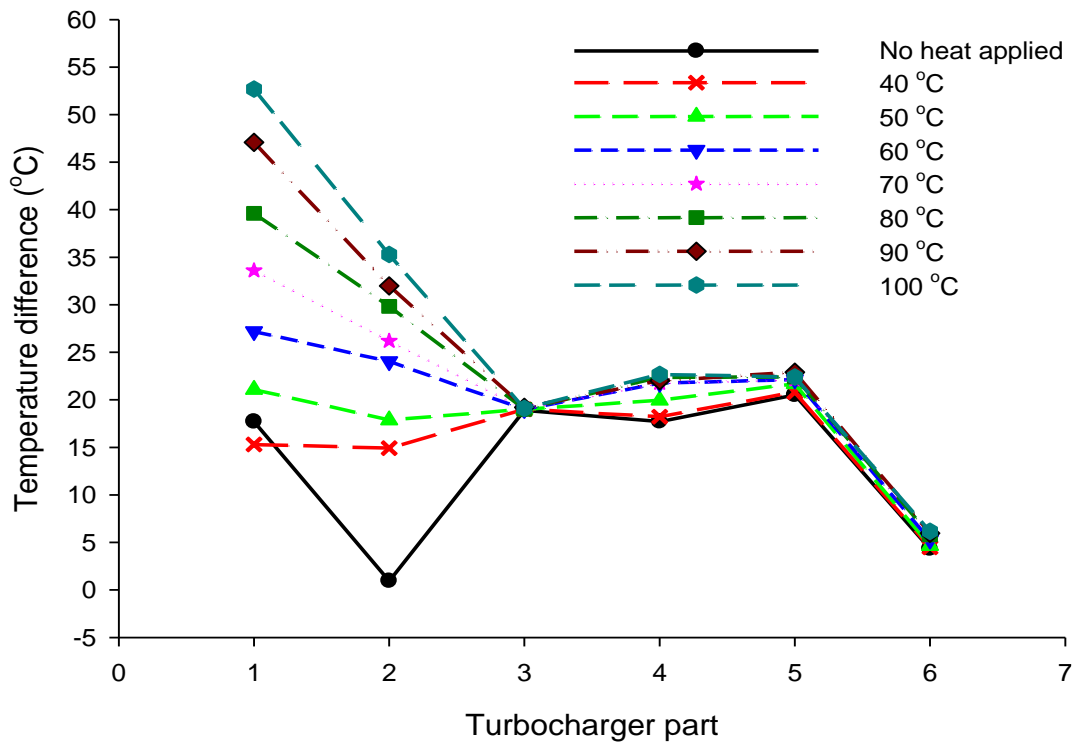


Fig. 8. Temperature difference across turbocharger components at 70 000rpm

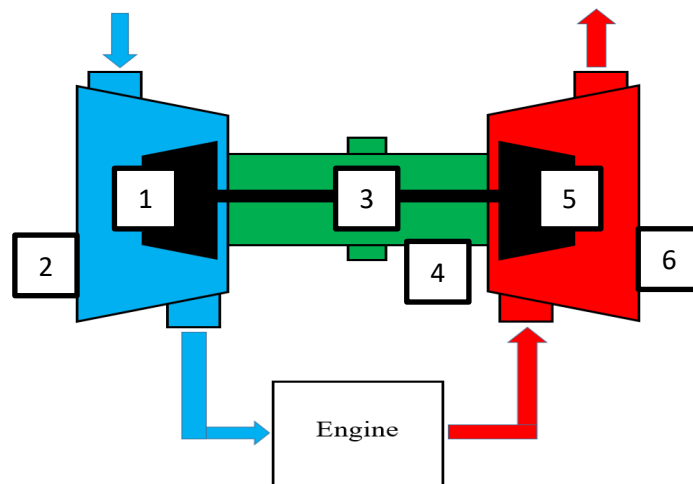


Fig. 9. Turbocharger parts schematic diagram

Table 2
 Turbocharger Parts Components

Number	Turbocharger parts
1	Turbine internal temperature difference
2	Turbine outer casing temperature difference
3	Lubricating oil temperature difference
4	Bearing housing outer temperature difference
5	Compressor internal temperature difference
6	Compressor outer casing temperature difference

Figure 10 shows the temperature difference across the turbocharger parts at constant turbine inlet temperature of 100 °C with varied turbocharger speed. From the figure, the variations of the temperature difference from the lubricating oil, bearing housing outer temperature difference, internal compressor temperature difference and compressor outer casing temperature difference can be observed. Observing the trends that shown at lubricating oil temperature difference, the variations of temperature difference are caused by the frictional force that generated between the thrust bearing inside the housing. While the turbocharger speed increase, the temperature difference will also increase due to the frictional force increment at the bearing. This heat will travel to the bearing housing thus causing the temperature difference occur at the outer bearing housing. The temperature difference that travels to the bearing housing from the bearings inside the bearing housing will combine with the temperature difference that travels from the turbine outer casing, thus causing the temperature difference at outer bearing housing will be higher compared to the temperature difference that generated by the lubricating oil. Other than that, the compressor side also generates temperature difference during the air compression process that happens inside the compressor casing. The temperature difference that produced will travels to the compressor outer casing.

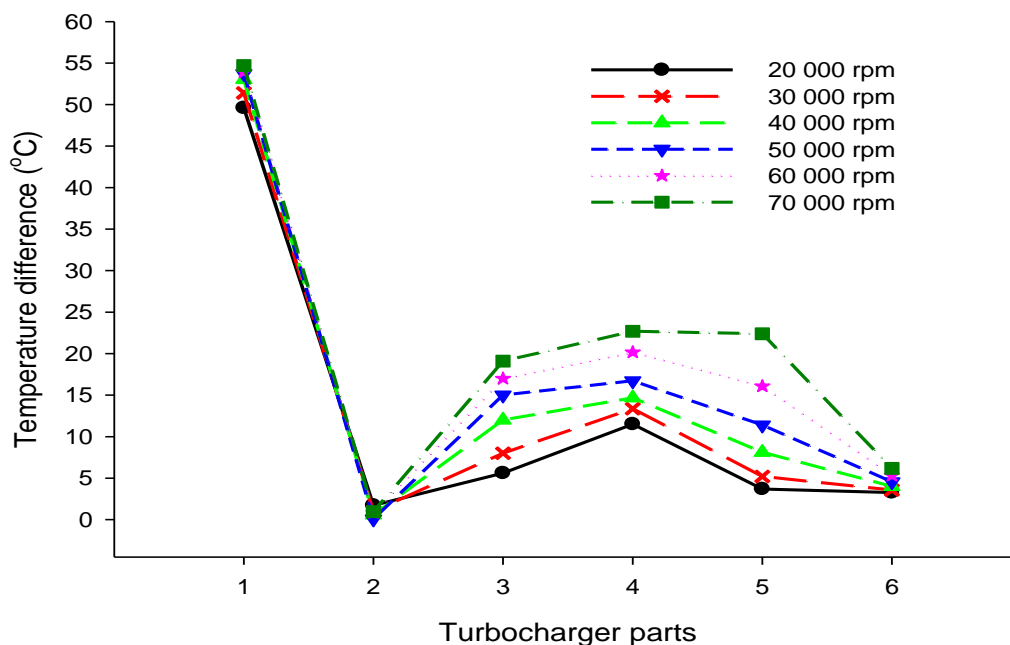


Fig. 10. Temperature difference across the turbocharger part at temperature 100°C in turbine inlet

Figure 11 shows the compressor mass flow rate on different turbine inlet temperature while the turbocharger speed is increase. From the figure, it can be seen that while the temperature at turbine inlet is at 40°C, the mass flow rate inside the compressor is 1.34% higher compared to the condition where no heat is applied to the turbine inlet. Next, when the turbine inlet temperature is set to 50°C, the mass flow rate is 0.04% higher compared to the mass flow rate at 40°C. When the turbine inlet temperature is increase to 60°C, the mass flow rate at compressor is 2.66% higher compared to the mass low rate at 50°C turbine inlet temperature. Moreover, while the temperature at turbine inlet is increase to the 70°C, the mass flow rate is 0.85% higher compared to the mass flow rate for turbine inlet temperature of 60°C. Next, when the temperature at turbine inlet is set to 80°C, the mass flow rate at compressor is 0.51% higher compared to the mass flow rate at turbine inlet temperature of 70°C. When the temperature at the turbine inlet is 90°C, the mass flow rate at the compressor is 0.61% higher compared to the compressor mass flow rate when the turbine inlet temperature is set to 80°C. Finally, when the temperature at turbine inlet is set to 100°C, the mass flow rate at compressor is 0.34% higher compared to the compressor mass flow rate when the turbine inlet temperature is set to 90°C. From Figure 11, it can be seen that the compressor mass flow is only affected by the temperature of the turbine inlet in a small percentage. This is shown by the percentage of difference between each mass flow rate line versus turbine inlet temperature where the percentage of difference is less than zero.

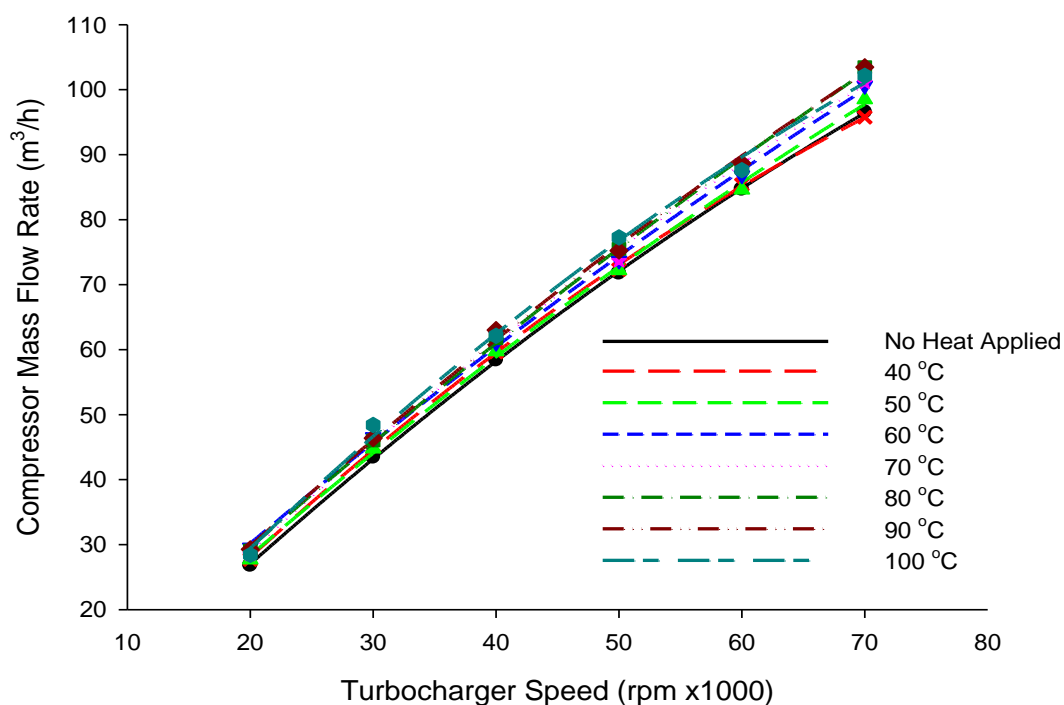


Fig. 11. Graph of compressor mass flow rate versus turbocharger speed on different turbine inlet temperature

4. Conclusions

In this paper, the study about heat propagation that started from turbine side to the bearing housing side and lastly to the compressor side of a turbocharger was investigated. In the experiment, six different turbocharger speed ranged from 20 000 rpm until 70 000 rpm and seven different turbine inlet temperature ranged from 40°C to 100°C was used as manipulated parameters where

the temperature difference at each measurement point was determined. From the results obtained, several conclusions were made.

- i. Turbine housing will extract the energy that contained inside the heated compressed air that enters the turbine housing. These conditions will cause the temperature at turbine outlet will be lower compared to the turbine inlet temperature.
- ii. Based on the temperature difference on each turbocharger components, the heat will propagate from turbine side to the bearing housing and finally to the compressor side through the outer casing of the turbocharger.
- iii. Heat inside the turbine side can be prevented to travel inside the internal bearing housing through the usage of turbine backplate at the turbine side.
- iv. The heat that reaches the compressor side gives small effect to the compressor mass flow where the percentage of difference between each mass flow rate line versus turbine inlet temperature shows less than zero in percentage of difference.

Acknowledgement

The authors would like to thank the Faculty of Mechanical and Automotive Engineering Technology, Universiti Malaysia Pahang Al-Sultan Abdullah (UMPSA) for providing the facilities to carry out this research, and Universiti Malaysia Pahang Al-Sultan Abdullah (UMPSA) for providing financial support under Internal Research grants PGRS190306 and RDU180391.

References

- [1] Malaysian Automotive Association. "Record Sales of New Motor Vehicles; TIV Surpassed 700,000 Unit Mark!." *Press Statement, Malaysian Automotive Association*, 2003.
- [2] Demir, Usame, Samet Çelebi, and Salih Özer. "Experimental investigation of the effect of fuel oil, graphene and HHO gas addition to diesel fuel on engine performance and exhaust emissions in a diesel engine." *International Journal of Hydrogen Energy* 52 (2024): 1434-1446. <https://doi.org/10.1016/j.ijhydene.2023.08.007>
- [3] Zhai, Cong, Yanqing Xu, Kening Li, Ronghui Zhang, Tao Peng, Changfu Zong, and Hongguo Xu. "Periodic intermittent cruise control: An innovative approach for reducing fuel consumption and exhaust emissions in road traffic systems." *Process Safety and Environmental Protection* 177 (2023): 1197-1210. <https://doi.org/10.1016/j.psep.2023.07.079>
- [4] Özer, Salih, and Erdiñç Vural. "The effect of the addition of H₂, H₂+ HHO and H₂+ HHO+ O₂ from the intake manifold on exhaust emissions in a diesel generator using diesel/toluene/diethyl ether as pilot fuel." *International Journal of Hydrogen Energy* 52 (2024): 1247-1260. <https://doi.org/10.1016/j.ijhydene.2023.04.122>
- [5] Bontempo, Rodolfo, Massimo Cardone, Marcello Manna, and Giovanni Vorraro. "Steady and unsteady experimental analysis of a turbocharger for automotive applications." *Energy Conversion and Management* 99 (2015): 72-80. <https://doi.org/10.1016/j.enconman.2015.04.025>
- [6] Serrano, José R., Pablo Olmeda, Francisco J. Arnau, Miguel A. Reyes-Belmonte, and Hadi Tartoussi. "A study on the internal convection in small turbochargers. Proposal of heat transfer convective coefficients." *Applied Thermal Engineering* 89 (2015): 587-599. <https://doi.org/10.1016/j.applthermaleng.2015.06.053>
- [7] Fridrichová, K., L. Drápal, J. Vopařil, and J. Dluhoř. "Overview of the potential and limitations of cylinder deactivation." *Renewable and Sustainable Energy Reviews* 146 (2021): 111196. <https://doi.org/10.1016/j.rser.2021.111196>
- [8] Ritzmann, Johannes, Norbert Zsiga, Christian Peterhans, and Christopher Onder. "A control strategy for cylinder deactivation." *Control Engineering Practice* 103 (2020): 104566. <https://doi.org/10.1016/j.conengprac.2020.104566>
- [9] Morris, Nick, Mahdi Mohammadpour, Ramin Rahmani, P. M. Johns-Rahnejat, Homer Rahnejat, and D. Dowson. "Effect of cylinder deactivation on tribological performance of piston compression ring and connecting rod bearing." *Tribology International* 120 (2018): 243-254. <https://doi.org/10.1016/j.triboint.2017.12.045>
- [10] Ji, Changwei, Ke Chang, Shuofeng Wang, Jinxin Yang, Du Wang, Hao Meng, and Huaiyu Wang. "Effect of injection strategy on the mixture formation and combustion process in a gasoline direct injection rotary engine." *Fuel* 304 (2021): 121428. <https://doi.org/10.1016/j.fuel.2021.121428>

- [11] Pratama, Raditya Hendra, Weidi Huang, Seoksu Moon, Jin Wang, Kei Murayama, Hiroyoshi Taniguchi, Toshiyuki Arima, Yuzuru Sasaki, and Akira Arioka. "Hydraulic flip in a gasoline direct injection injector and its effect on injected spray." *Fuel* 310 (2022): 122303. <https://doi.org/10.1016/j.fuel.2021.122303>
- [12] Park, Sangjae, Ji Yong Shin, Choongsik Bae, Jinyoung Jung, and Juhun Lee. "Combustion phenomena affecting particle emission under boosting conditions in a turbocharged gasoline direct injection engine." *Fuel* 286 (2021): 119362. <https://doi.org/10.1016/j.fuel.2020.119362>
- [13] Demir, Usame, Gokhan Coskun, Hakan S. Soyhan, Ali Turkcan, Ertan Alptekin, and Mustafa Canakci. "Effects of variable valve timing on the air flow parameters in an electromechanical valve mechanism-A CFD study." *Fuel* 308 (2022): 121956. <https://doi.org/10.1016/j.fuel.2021.121956>
- [14] Gong, Zhen, Liyan Feng, and Zixin Wang. "Experimental and numerical study of the effect of injection strategy and intake valve lift on super-knock and engine performance in a boosted GDI engine." *Fuel* 249 (2019): 309-325. <https://doi.org/10.1016/j.fuel.2019.03.005>
- [15] Adedeji, Bukola Peter. "Electric vehicles survey and a multifunctional artificial neural network for predicting energy consumption in all-electric vehicles." *Results in Engineering* 19 (2023): 101283. <https://doi.org/10.1016/j.rineng.2023.101283>
- [16] Tung, Nguyen Thanh, and Luong Van Van. "Modeling to study the braking efficiency of the electric vehicle." *Materials Today: Proceedings* (2023).
- [17] Ruth, John C., and Gregory Stephanopoulos. "Synthetic fuels: what are they and where do they come from?." *Current Opinion in Biotechnology* 81 (2023): 102919. <https://doi.org/10.1016/j.copbio.2023.102919>
- [18] Abdelmajid, Chehhat, Si-Ameur Mohamed, and Boumeddane Boussad. "CFD analysis of the volute geometry effect on the turbulent air flow through the turbocharger compressor." *Energy Procedia* 36 (2013): 746-755. <https://doi.org/10.1016/j.egypro.2013.07.087>
- [19] Chiong, M. S., S. Rajoo, R. F. Martinez-Botas, and A. W. Costall. "Engine turbocharger performance prediction: One-dimensional modeling of a twin entry turbine." *Energy Conversion and Management* 57 (2012): 68-78. <https://doi.org/10.1016/j.enconman.2011.12.001>
- [20] Burke, R. D., C. D. Copeland, and Tomasz Duda. "Investigation into the assumptions for lumped capacitance modelling of turbocharger heat transfer." In 6th International Conference on Simulation and Testing. 2014.
- [21] Burke, Richard D., Chris R. M. Vagg, David Chalet, and Pascal Chesse. "Heat transfer in turbocharger turbines under steady, pulsating and transient conditions." *International Journal of Heat and Fluid Flow* 52 (2015): 185-197. <https://doi.org/10.1016/j.ijheatfluidflow.2015.01.004>
- [22] Burke, R. D., P. Olmeda, F. J. Arnau, M. Reyes-Belmonte, and CMT-Motores Térmicos. "Modelling of turbocharger heat transfer under stationary and transient engine operating conditions." In *Institution of Mechanical Engineers-11th International Conference on Turbochargers and Turbocharging*, pp. 103-112. 2014. <https://doi.org/10.1533/978081000342.103>
- [23] Serrano, Jose, Pablo Olmeda, Francisco Arnau, Miguel Reyes-Belmonte, and Alain Lefebvre. "Importance of heat transfer phenomena in small turbochargers for passenger car applications." *SAE International Journal of Engines* 6, no. 2 (2013): 716-728. <https://doi.org/10.4271/2013-01-0576>
- [24] Serrano, Jose, Pablo Olmeda, Francisco Arnau, and Artem Dombrovsky. "General procedure for the determination of heat transfer properties in small automotive turbochargers." *SAE International Journal of Engines* 8, no. 1 (2015): 30-41. <https://doi.org/10.4271/2014-01-2857>
- [25] Gao, Xunan, Bojan Savic, and Roland Baar. "A numerical procedure to model heat transfer in radial turbines for automotive engines." *Applied Thermal Engineering* 153 (2019): 678-691. <https://doi.org/10.1016/j.applthermaleng.2019.03.014>
- [26] Prévost, F., Y. Le Moual, A. Maiboom, X. Tauxia, T. Payet-Burin, and O. Davodet. "An analytical user-friendly methodology to transform compressor and turbine supplier characterization maps dedicated to 1D engine simulation: Modelling of turbocharger heat transfer and friction losses." *Applied Thermal Engineering* 221 (2023): 119812. <https://doi.org/10.1016/j.applthermaleng.2022.119812>
- [27] Serrano, José Ramón, Pablo Olmeda, Francisco J. Arnau, Artem Dombrovsky, and Les Smith. "Turbocharger heat transfer and mechanical losses influence in predicting engines performance by using one-dimensional simulation codes." *Energy* 86 (2015): 204-218. <https://doi.org/10.1016/j.energy.2015.03.130>
- [28] Salameh, Georges, Guillaume Goumy, and Pascal Chesse. "Water cooled turbocharger heat transfer model initialization: Turbine and compressor quasi-adiabatic maps generation." *Applied Thermal Engineering* 185 (2021): 116430. <https://doi.org/10.1016/j.applthermaleng.2020.116430>